6.1 THE INFLUENCE OF BOUNDARY LAYER STRUCTURE ON RURAL OZONE OBSERVED DURING PROPHET 2001 AND 2001 SUMMER INTENSIVES

Mark A. R. Lilly*, Jennie L. Moody, Anthony J. Wimmers
Department of Environmental Sciences
University of Virginia

Mary A. Carroll
Department of Atmospheric, Oceanic, and Space Sciences
University of Michigan

Troy D. Thornberry
Department of Chemistry, University of Toronto

Leah Yageman, Michelle L'Heureux, Michael Mitchell, Curtis Seaman, Edward Fortner
NSF REU Students, University of Michigan Biological Station,
Douglas Lake, Michigan

1. INTRODUCTION

The Program for Research on Oxidants: Photochemistry, Emissions, and Transport (PROPHET) have been making continuous measurements of ozone during atmospheric chemistry intensives in July and August of 1998, 2000, and 2001. For the past two summers, 2000 and 2001, an Integrated Sounding System (ISS) from NCAR (National Center for Atmospheric Research) has been deployed to provide detailed measurements of boundary layer structure. Understanding boundary layer structure at this rural, forested site in Northern Michigan is a key part of the PROPHET mission to investigate the fundamental processes that determine atmospheric levels of ozone. Investigating the evolution and structure of the boundary layer under different synoptic scale meteorological patterns has improved our understanding of diurnal ozone behavior (Figure 1).

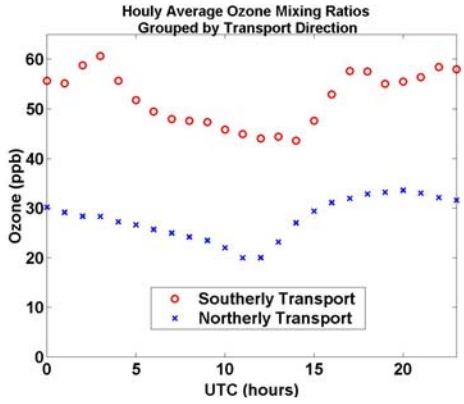

Figure 1. Hourly average ozone mixing ratios over the course of a day, for days grouped according to transport direction

Back trajectories were calculated with the HYSPLIT 4 (Hybrid Single-Particle Langrangian Integrated Trajectory) model (Draxler and Hess, 1997). These trajectories were analyzed and separated into transport direction for 1998 and 2000. During the PROPHET 1998 intensive campaign northerly flow out of Canada was observed 44% of the time, while southerly was observed 16% of the time (Cooper, 2001). The analysis of PROPHET 2000 back trajectories revealed a similar flow pattern, northerly flow was observed 45% of the time, while the southerly flow was observed for 18% of the campaign. Typically, when the PROPHET site is on the backside of a surface anticyclone the site receives a modified maritime-sub-tropical air mass from the south/southwest and these are the trajectories that exhibit a pronounced increase in ozone concentrations. In addition to these obvious changes that are driven by source region (eg., 25 ppb increase in average ozone, Figure 1), we are interested in how the physical characteristics of the atmosphere change under different flow patterns, and how these changes affect trace gas chemistry. A study by Crespi′ et al. (1994), using temperature profiles from free and tethered balloons, found that synoptic conditions exert a strong influence on the daily boundary layer height. We show similar results and go one step further, demonstrating how changes in boundary layer behavior can influence ozone concentrations.

Corresponding author address: Mark A.R. Lilly, Dept. of Environmental Sciences, Clark Hall, Univ. of Virginia, Charlottesville, VA, 22903; email: ml3x@virginia.edu

2. INSTRUMENTATION AND MEASUREMENTS

NCAR's ISS consists of a 915 MHz wind profiler, RASS (radio acoustic sounding system), a 10-meter meteorological tower, and the capability to obtain atmospheric profiles using free rawinsondes and tethered rawinsondes. The individual components of the ISS, integrated with one another, can provide detailed measurements of the atmospheric boundary layer. The 915 MHz Doppler Beam Swinging (DBS) wind profiler measures the Doppler power spectrum using six alternating beam positions. The six alternating beam positions consist of four oblique beams and two vertical beams of orthogonal polarizations. The vertical beam measurements are made in between each alternating oblique beam measurement (Cohn and Angevine, 1999). There were nine sweeps per cycle, with each sweep lasting approximately thirty seconds. The profiler was in low mode for the first eight sweeps and then made one high mode measurement at the end of each cycle. The low mode measurements give better resolution close to the ground, while the one high mode measurement measures higher into the vertical, but loses resolution between gates. A time averaged Doppler power spectrum for each range gate is computed before the moments of the signal can be calculated (Carter et al., 1995). The zeroth moment of the Doppler spectrum is the signal power, the first moment is the mean Doppler velocity, and the second moment is the spectrum variance. The profiler measures the radial component of the wind in each beam direction. A consensus-average over a 25-minute period, at each range gate, and each beam position of the radial velocities is taken before the average horizontal wind vector can be calculated (Carter et al., 1995). The vertical beams provide a direct measurement of the vertical velocity

The wind profiler is a very sensitive long-waved Doppler radar that detects gradients in the refractive index (Angevine et al., 1998). Turbulence can be responsible for producing variations in temperature, humidity and pressure, which cause a change in the refractive index (Dye et al., 1995). Variations in the refractive index are caused by turbulence that is spatially one-half the profiler's wavelength (15 cm) and these regions of small-scale turbulence are responsible for the incident power return to the wind profiler (Frisch and Weber, 1991; Angevine et al., 1994a). The profiler signal-to-noise ratio (SNR) of the returned backscatter power is related to refractive index structure parameter, Cn^2 (White et al., 1991). Peaks in the refractive index structure parameter correspond to top of the boundary layer (Wyngaard and LeMone, 1980), therefore range corrected SNR should indicate the top of the boundary layer due to this relationship between SNR and Cn^2 (Angevine et al., 1994a). Because the profiler's signal drops off as $1/r^2$, the SNR needs to be range corrected as follows:

$$snr + 10 * \log_{10}(range)^2 \qquad (1)$$

Figure 2 shows the range corrected SNR of the vertical beam. An automated algorithm to find the top of the convective boundary layer (CBL) was implemented and is depicted as the solid black line in Fig. 2 (Angevine et al., 1994; Angevine et al., 1998). The algorithm finds the maximum range corrected SNR value for each vertical profile and then computes a half-hour running mean of the heights that correspond to those maximum range corrected SNR values.

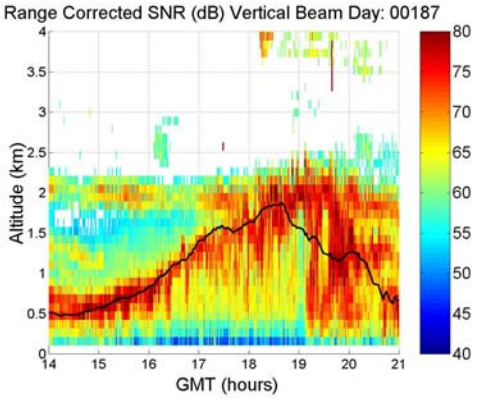

Figure 2. The range corrected SNR from the vertical beam and dark line is the automated algorithm

---

The wind profiler technology used in combination with RASS provides a technique to obtain virtual temperature profiles every half-hour. An acoustic pulse sent vertically by four loud speakers surrounding the profiler, is tracked by the vertical beam of the radar. The vertical beam of the radar measures the speed of the vertically propagating acoustic wave front through the atmosphere (Angevine et al., 1994b). The speed of the wave is influenced by the fluctuations of air density through which the wave is traveling. From the relationship of the speed of sound through the median and the vertical wind speed, a vertical profile of virtual temperature is derived (Angevine et al., 1994b).

$$T_v(^oC) = \frac{(C_a - w)^2}{401.92} - 273.16 \qquad (2)$$

where C_a is the measured speed of sound and w is the vertical wind speed measured by the profiler

3. LIMITATIONS OF ISS

A limiting factor of following the early development of the nocturnal boundary layer (NBL) is the height of the profiler and RASS first gate. The wind profiler measures at 46 range gates that are separated by 105 m. The first gate of the profiler is 105 m above ground level (AGL). The RASS measures at 25 range gates, each separated by 60 m. The first gate of the RASS is 120 m above ground level. RASS derived virtual temperature profiles are more useful than the range corrected SNR in determining the height of the NBL. The automated algorithm using the range corrected SNR continues to find peaks in SNR well above the decaying CBL and the evolving NBL, in the residual layer, as long as there is turbulence inducing refractive index fluctuations on the order of one-half the profiler's wavelength (15 cm) (Angevine, et al. 1994a). The automated algorithm using the vertical beam of the profiler does well in capturing the growth of the CBL. However, the RASS signal falls off with height and the highest RASS gate is at only 1560 m which, on some days, may be to low to detect the top of the CBL. Another limitation of using RASS to determine the CBL is that the less stable afternoon atmospheric profiles cause the acoustic pulse of the RASS to be "blown" horizontally not allowing for detection by the vertical beam of the radar (Angevine et al., 1998).

4. OTHER METHODS USED IN DETERMINING BOUNDARY LAYER HEIGHT

Using data collected by the ISS, various other methods have been examined to help in the identification of features existing in the NBL and the early morning evolution of the CBL. A method to calculate the lifted condensation level (LCL) height (Stull, 1998), calculation of potential and equivalent potential temperature profiles, calculation of the gradient Richardson number and the bulk Richardson number (Pleim and Xiu, 1995; Grimsdell and Angevine, 1998), and free rawinsonde and tethered rawinsonde profiles have been used in combination with the automated algorithm to determine boundary layer heights throughout the day. Along with the automated algorithm suggested by Angevine (1994a), Dye (1995) describes another algorithm in which the median Cn^2 at each gate over a chosen period is calculated. This alternate algorithm has also been used in determining boundary layer height.

The presence of clouds complicates the interpretation of the automated algorithm to find the height of the CBL (Angevine et al, 1994a) and cloudy boundary layers are typically not well understood (Stull, 1988; Grimsdell and Angevine, 1998). The PROPHET site is surrounded by Lake Michigan to the north and west and Lake Huron to the north and east. These large bodies of water as well as a number of smaller lakes account for a lake-induced stratus layer that the site experiences periodically. The temperature and pressure of the LCL has been calculated using surface meteorological data as described by Stull (1998) with modifications according to Betts (2001). Using the hypsometric equation, the height of the LCL was calculated. The height of the LCL will be assumed to be in close proximity to cloud base and will compared to the running mean of the range corrected SNR.

Potential temperature and equivalent potential temperature profiles derived from the RASS profiles of virtual temperature will be used to identify features of the NBL and the early morning evolution of the CBL. Figure 3 is a vertical profile of potential temperature that has been calculated from the virtual temperature and surface meteorological measurements. Figure 3 illustrates the evolution of the NBL from just after 00Z until the CBL begins to grow into the NBL just before 15Z.

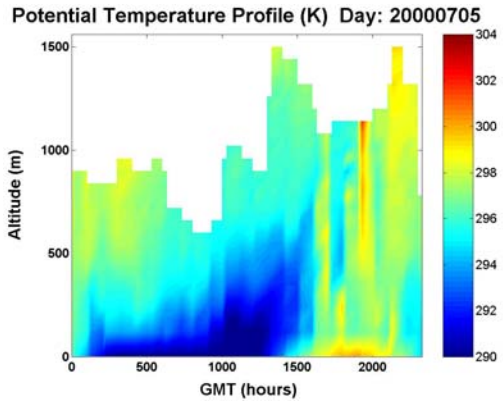

Figure 3. Potential Temperature Profile

The calculation of Richardson number and Bulk Richardson number will be used to identify the stability of the atmosphere within the NBL and the elevated residual layer. The difference between the two calculations is that Pleim and Xiu's (1995) method for the calculation of the bulk Richardson number involves only one wind measurement in the calculation, while the gradient Richardson number calculation involves the wind shear across a layer.

Pleim and Xiu's (1995) method of representing the planetary boundary layer bulk Richardson number is calculated by:

$$Rib = \frac{gz\Delta\theta v}{\overline{\theta v}(u(z)^2 + v(z)^2)} \quad (3)$$

where g is the gravitational force, z is the altitude (height AGL of current profiler gate), θv is the virtual potential temperature, and u and v are the components of the horizontal wind. Pleim and Xiu (1995), as well as Grimsdell and Angevine (1998) describe the following relationships for use in equation 3:

$\Delta\theta v = \theta v(z) - \theta vs$ and $\overline{\theta v} = 0.5[\theta v(z) + \theta vs]$

5. CONCLUDING REMARKS

The depth of the boundary layer is one of those fundamental properties that influence fluctuating trace gas mixing ratios. Understanding the time varying behavior of ozone and other trace gases is the mission of the ongoing PROPHET campaign. Determining the depth and evolution of the CBL and the NBL under all types of atmospheric conditions is the first challenging step in relating the chemistry to the physics of the boundary layer. Many different methods and calculations have been used in combination to obtain a breakdown of boundary layer height under varying synoptic meteorological conditions. These results will be presented along with daily ozone data also categorized by synoptic patterns to illustrate the influence of boundary layer structure on observed chemical behavior.

5. REFERENCES

Angevine, W. M., A. B. White, S. K. Avery, 1994a: Boundary-Layer depth and entrainment zone characterization with a boundary-layer profiler, Bound.-Layer Meteor., 68, 375-385.

Angevine, W. M., W. L. Ecklund, D. A. Carter, K. S. Gage, K. P. Morgan, 1994b: Improved radio acoustic sounding techniques, J. Atmos. Oceanic Technol., 11, 42-49.

Angevine, W. M., A. W. Grimsdell, L. M. Hartten, A. C. Delany, 1998: The flatland boundary layer experiments, Bull. Amer. Meteor. Soc., 79, 419-431.

Betts, A. K., J. D. Fuentes, M. Garstang, J. H. Ball, 2001: Surface diurnal cycle and boundary layer structure over Rondonia during the rainy season, J. Geophys. Res. (in press).

Carter, D. A., K. S. Gage, W. L. Ecklund, W. M. Angevine, P. E. Johnston, A. C. Riddle, J. Wilson, C. R. Williams, 1995: Developments in UHF lower tropospheric wind profiling at NOAA's Aeronomy Laboratory, Radio Science, 30, 977-1001.

Cohn, S. A., W. M. Angevine, 1999: Boundary layer height and entrainment zone thickness measured by lidars and wind profiling radars, J. Appl. Meteor., 39, 1233-1247.

Cooper, O. R., 2001: PROPHET'98 meteorological overview and air-mass classification, J. Geophys. Res., 106 (D20), 24289-24299.

Crespi′, S. N., B. Arti′nano, H. Cabal, 1995: Synoptic classification of the mixed-layer height evolution, J. Appl. Meteor., 34, 1666-1677.
Draxler, R. R., G. D. Hess, 1997: Description of the Hysplit_4 modeling system, NOAA Tech Memo ERL ARL-224, Dec, 24p.

Dye, T. S., C. G. Linsey, J. A. Anderson, 1995: Estimates of mixing depths from boundary layer radar profilers, 1995 AMS Ninth Symposium on Meteorological Observations and Instrumentation.

Frisch, A. S., B. L. Weber, 1991: Notes and Correspondence: The distribution of Cn^2 as measured by 50-, 405-, and 915-MHz wind profilers, J. Atmos. Oceanic Technol., 9, 318-322.

Grimsdell, A. W., W. M. Angevine, 1998: Convective boundary layer height measurement with wind profilers and comparison to cloud base, J. Atmos. Oceanic Technol., 15, 1331 - 1338.

Pleim, J. E., A. Xiu, 1995: Development and testing of a surface flux and planetary boundary layer model for application in mesoscale models, J. Appl. Meteor., 34, 16-32.

Stull, R. B., An introduction to boundary-layer meteorology, Kluwer, 1998.

White, A. B., C. W. Fairall, D. W. Thomson, 1991: Radar Observations of humidity variability in and above the marine atmospheric boundary layer, J. Atmos. Oceanic Technol., 8, 639-658.

Wyngaard, J. C., M. A. LeMone, 1980: Behavior of the refractive index structure parameter in the entraining convective boundary layer, J. Atmos. Sci., 37, 1573-1585.